A&A 420, 1117–1121 (2004)
DOI: 10.1051/0004-6361:20034382
© ESO 2004

Astronomy & Astrophysics

Radius variations over a solar cycle

C. L. Selhorst[1], A. V. R. Silva[2], and J. E. R. Costa[1]

[1] CRAAM, Instituto Nacional de Pesquisas Espaciais, São José dos Campos, SP 12201-970, Brasil
[2] CRAAM, Universidade Presbiteriana Mackenzie, São Paulo, SP 01302-907, Brasil

Received 23 September 2003 / Accepted 2 March 2004

Abstract. We report the analysis of solar radius determination for more than 3800 maps at 17 GHz from the Nobeyama Radioheliograph (NoRH) over a solar cycle (1992–2003). The aim of this work is to determine the radius dependence on solar activity at 17 GHz. This study was divided into two parts: (i) the mean solar radius calculated using the coordinates around the solar limb, and (ii) the mean polar radius using only the coordinates within ±30° of the poles. While a good correlation between the mean solar radius and the sunspot number was found, the polar radius variations were found to be anti-correlated with sunspot number during this period. Nevertheless, the results showed the polar radius to have the same temporal evolution as the polar limb brightening at 17 GHz throughout the solar cycle, indicating a close relationship between them. A variation of 3″ was found for the mean radius from minimum to solar maximum, while the polar radius presented a variation of 1″ during the same period. Moreover, the distribution of center-to-limb distances showed a large increase in the equatorial regions with a double peaked profile during periods of maximum activity. From this work, we have concluded that the measurements of the solar radius at radio frequencies are influenced by various solar features, which make the definition of the solar radius a difficult task. Despite this, the study of solar radius is able to provide a good indication of the changes in the solar atmosphere.

Key words. Sun: fundamental parameters – Sun: atmosphere – sunspots

1. Introduction

Due to its importance in the calibration of the structure of solar atmospheric models, the solar radius has been measured at many different wavelengths. Over the last two decades, however, observations have shown the optical radius to vary over the period of a solar cycle, with measurements varying from some tens of milliarcsecs to approximately 0.5 arcsec. Anti-correlated variations with solar cycle indicators, such as sunspots, were found by Gilliland (1981), Wittmann et al. (1993), Delache et al. (1993), and Laclare et al. (1996). Nevertheless, Ulrich & Bertello (1995), Rozelot (1998), and Emilio et al. (2000) found a positive correlation between the activity cycle and the solar radius. Furthermore, Neckel (1995), Antia (1998), and Brown & Christensen-Dalsgaard (1998) report no variations in the solar radius correlated with the solar cycle in their observations.

Measurements of solar radius variations at radio frequencies represent changes in the position of the atmosphere where most part of the emission at these frequencies are formed, i.e., they reflect the changes in the local distribution of temperature and density. Nevertheless, very few studies have been made in this way. Bachurin (1983) reported an increase in the solar radius of nearly 9.6 and 13.8 arcsec at 13 and 8 GHz, respectively, from 1976 to 1981. More recently, Costa et al. (1999) measured the solar radius at 48 GHz and found the decrease in solar radius to be correlated with the solar cycle between 1991 and 1993. Moreover, a good correlation with the solar irradiance was found. This result is very important because solar irradiance variations may produce climate changes on Earth.

Here we present a study of the solar radius at 17 GHz using daily maps from the Nobeyama Radioheliograph (NoRH, Nakajima et al. 1994) during approximately one solar cycle (1992–2003). The method used in the data analysis and the results are presented in the next section. Implications from the results and the conclusions are discussed in Sects. 3 and 4, respectively.

2. Data analysis and results

In this work, we have analyzed over 3800 daily maps of the Sun at 17 GHz from the NoRH, over approximately one solar cycle (1992–2003). From each map, we determined the solar radius as explained below. An example of a solar map at 17 GHz during periods of minimum activity is shown in Fig. 1.

To calculate the solar radius, we first need to define the brightness temperature of the quiet Sun, which is taken as the most common temperature in each synthesized map. This temperature is nearly 10^4 K in every map, because NoRH solar maps are normalized to this temperature (Shibasaki 1998). Second, brightness distribution profiles across the disc are extracted by making radial cuts through the center of the

Send offprint requests to: C. L. Selhorst,
e-mail: caius@craam.mackenzie.br

Article published by EDP Sciences and available at http://www.aanda.org or http://dx.doi.org/10.1051/0004-6361:20034382

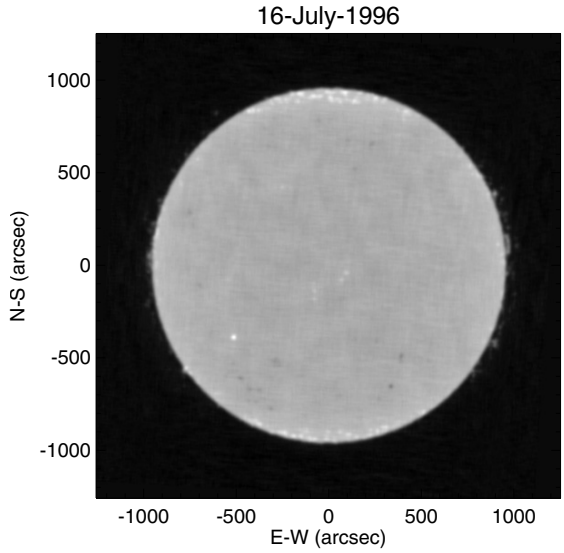

Fig. 1. Solar map from NoRH at 17 GHz observed on July 16, 1996, a period of minimum activity.

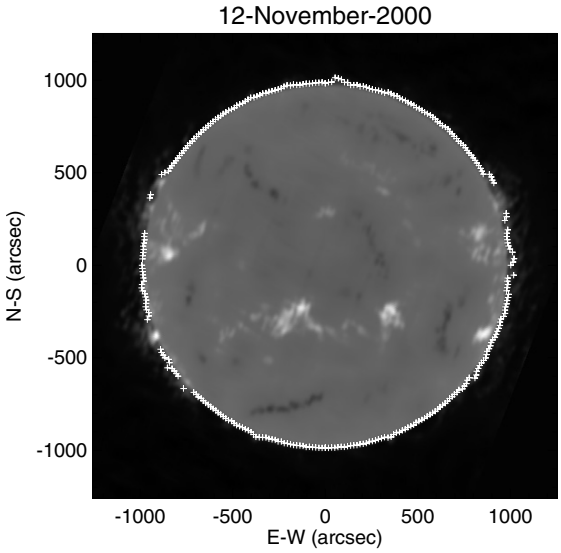

Fig. 3. Solar map during the maximum activity period showing the coordinates (crosses) used in the final circumference fit.

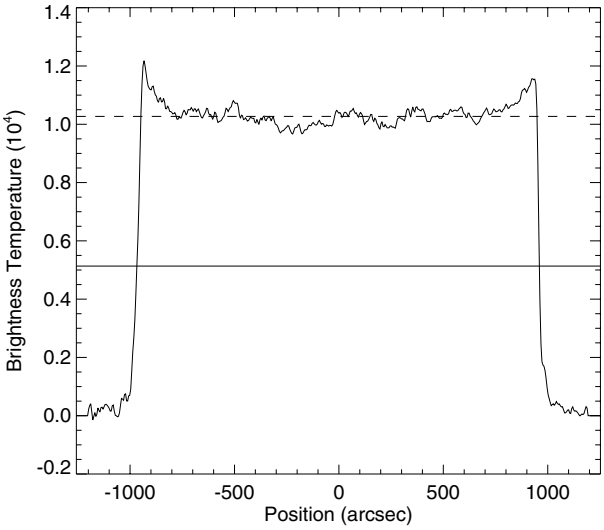

Fig. 2. Brightness temperature profile taken across the equatorial region of the map in Fig. 1. The dashed line represents the quiet Sun temperature and the solid line is equal to half of the quiet Sun (limb measurement position).

image, taken 1° apart. Figure 2 shows a typical profile, where the dashed line represents the quiet Sun brightness temperature and the solid line, its half value. Each cut yield a brightness profile. Following Costa et al. (1999), the solar limb was defined as the position where the brightness temperature is equal to half the value of the quiet Sun brightness temperature (solid line in Fig. 2).

Using the procedure described above, a total of 360 limb points were obtained for each solar image. Then, these were fit by a circumference that provided the center coordinates and the radius for each map. This radius, however, is influenced by the presence of active regions near the limb. To reduce this influence, a new circumference is fit considering only the coordinates that are within ±30 arcsec with respect to the previous radius. Once more, the standard deviation of all 360 points was measured with respect to the second radius fit, and the points with a discrepancy larger than ±30 arcsec were discarded and a new fit was made. This procedure is repeated at least 50 times or until the mean uncertainty of the new fit in comparison to the last fit differs by less than 0.025 arcsec, or if the number of points is smaller than 100. When this procedure is completed, most limb regions associated with active regions have been eliminated. The remaining points for one such image can be seen as the white crosses in Fig. 3. The implications of varying the 30″ tolerance criteria are discussed in Sect. 3.

All radii were measured using at least 258 limb points with a mean of 338 points and the mean of all uncertainties was found to be 6.1 arcsec. Despite correcting all values of the solar radius to 1 AU, an oscillation with a period of 1 year was detected, which may be due to the variation of the B_0 angle. The oscillation associated with the period of 1 year was eliminated by subtraction of a sine wave. After subtraction, the mean radius at 17 GHz was found to be 976.6 ± 1.5 arcsec. The results for one solar cycle, from 1992 to 2003, are plotted in Fig. 4a.

To verify the existence of a correlation with solar activity, we compare the radius results with the temporal variation of sunspot number. A running mean taken every 30 days of the mean radius and sunspot number are plotted in Figs. 4a and 4b, respectively. As can be seen from the figure, the radius at 17 GHz has a very good correlation with the sunspot number, with a correlation coefficient of 0.88. This coefficient is very significant due to the great number of data points (3820) used in the correlation.

To study the angular variation of the solar limb, we have compared maps during periods of maximum activity with those taken during periods of minimum activity. The distance from the limb position to Sun center was determined for each position angle (measured counter-clockwise with respect to the West equator), also at the location of half the quiet Sun value. This resulted in a distribution of 360 center-to-limb distances per map, for 10 maps made during the month of August 1996, a period of minimum activity. From the 10 maps, a mean value of

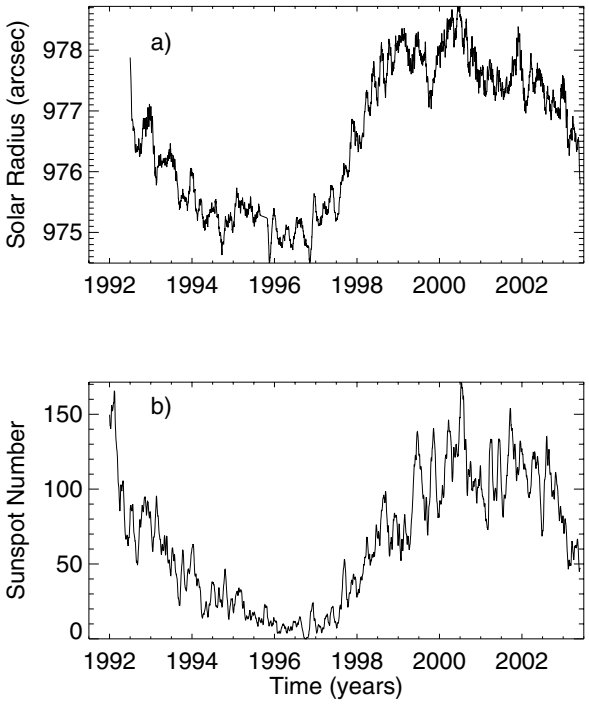

Fig. 4. A running mean taken every 30 days of the mean radius **a)** and sunspot number **b)**.

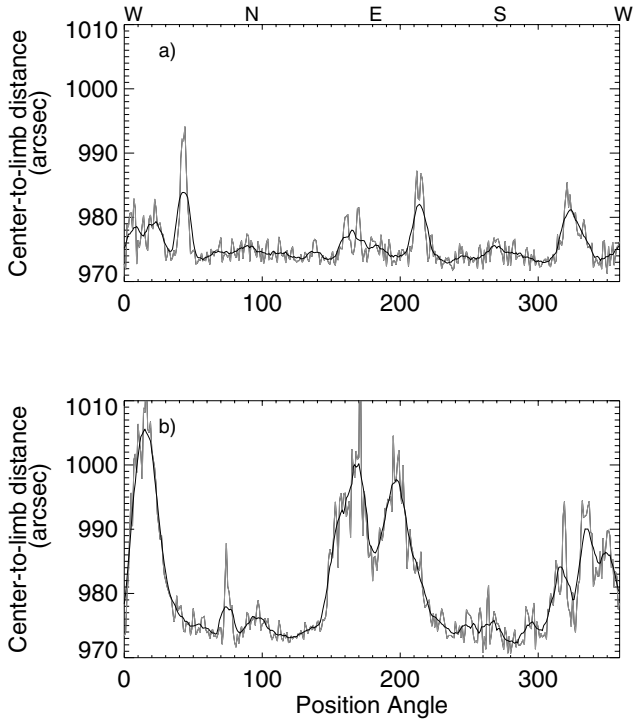

Fig. 5. Angular variation of the center-to-limb distance as a function of position angle for a mean of 10 maps during periods of **a)** minimum and **b)** maximum solar activity. The thick line represents a running mean of 10 points in both panels. In the figure, 90° and 270° correspond to the North and South poles, respectively, whereas the East and West equator are given by 180° and 360°.

the center-to-limb distance for each position angle was calculated. In Fig. 5a we plot the averaged center-to-limb positions as a function of position angle. The same procedure was repeated for 10 maps made during the month of August 2000, a period of maximum solar activity. The results shown in Fig. 5b make evident the large increase in the solar radius near equatorial regions during maximum activity in comparison with those during quiet periods. This difference may be caused by the larger number of solar features, such as active regions and proeminences, that are more common during periods of maximum solar activity. Nevertheless, the center-to-limb distances of the polar region were approximately the same during both periods.

Due to the result presented above, the temporal evolution of the polar radius was calculated using all the maps during one solar cycle. In this study, just the 122 points taken between 60° and 120°, and between 240° and 300° position angles were considered. Once more, we used a recurrent fit of a mean circumference discarding in each fit the points with more than ±15 arcsec with respect to the previous adjust. In this procedure, the minimum number of points used in the fit of the mean circumference was 40 points.

The mean of all uncertainties in the sample was found to be 2.2 arcsec. After removal of the periodic oscillation close to 1 year by subtracting a sine function, the mean polar radius obtained was 974.4 ± 0.8 arcsec. A running mean taken every 30 days of the measured polar radius and sunspot number over one solar cycle are shown in Fig. 6 (a and c respectively). An anti-correlation between the polar radius and sunspot number is clearly seen, with a correlation coefficient of −0.64.

In a previous study of polar limb brightening seen in 17 GHz solar maps, Selhorst et al. (2003) concluded that the intensity of this brightening was anti-correlated with the solar cycle. For comparison, a 30 day running mean of the North polar limb brightening is plotted in Fig. 6b. A good coincidence in the temporal variation of the polar limb brightening and the polar radius is clearly seen, with a correlation coefficient of 0.63. A very intense brightening (30–40%), confined in a region near the polar limb may cause the image of the Sun at half-power to be stretched outward in those locations due to the convolution of the telescope synthesized beam (10″) and the polar brightened Sun, thus increasing the value of the measured polar radius.

3. Discussion

In the analysis of the 17 GHz maps, we have found two different behaviors for the radius: (i) when all positions (except those within active regions) around the solar limb are considered, a good correlation (correlation coefficient of 0.88 for 3820 maps) with sunspot number was obtained; whereas (ii) an anti-correlation (correlation coefficient of −0.64) with solar activity was found in the case where only the polar limb coordinates were taken into account in the polar radius determination. These apparently discrepant results can be explained by changes in the equatorial solar atmosphere during the period of maximum activity that cause an increase in the solar radius. This solar radius increment is double peaked near the equator (as seen in Fig. 5b). Even though the solar poles are less affected by the solar maximum activity, they are the

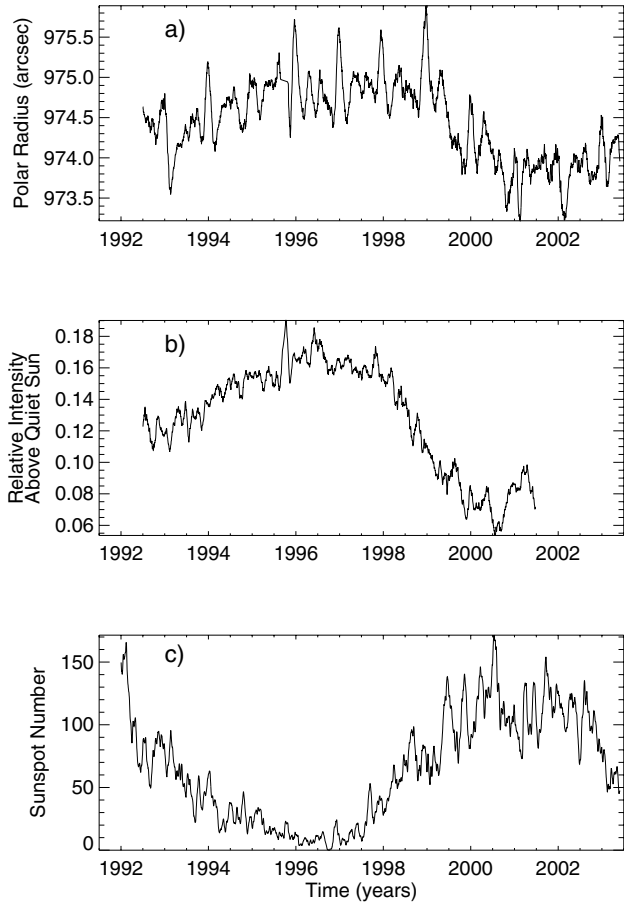

Fig. 6. A running mean taken every 30 days of the **a)** polar radius, **b)** mean intensities of the brightness temperature above the quiet Sun level at the North pole, and **c)** sunspot number for the same period.

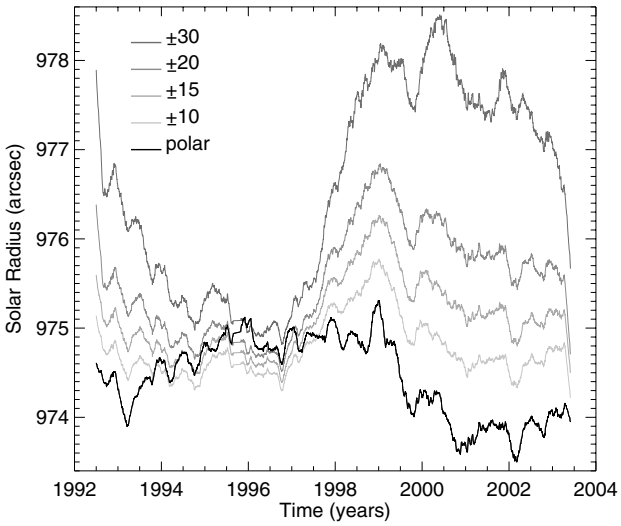

Fig. 7. Comparison between a running mean taken every 100 days of the solar radius fit for different deviation criteria, plus the polar radius (as a black line). The criteria are identified in the figure with varying gray scale colors.

Table 1. The mean radius for different deviation criteria, the minimum and mean number of points used in the fits, the correlation coefficient between the radius variation and the sunspot number, and the last column shows the correlation coefficient between the radius variation and the North polar limb brightening.

	Radius	# Points		Correl. coefficient	
		Min.	Mean	Sunspot	Bright.
±30	976.6 ± 1.5	258	338.1	0.88	–0.85
±20	975.5 ± 0.9	236	324.9	0.69	–0.67
±15	975.1 ± 0.7	218	317.2	0.47	–0.50
±10	974.8 ± 0.6	154	308.0	0.19	–0.24
polar	974.4 ± 0.8	91	120.5	–0.64	0.63

location of significant limb brightening at 17 GHz, that increases during solar minimum (Selhorst et al. 2003). This indicates that the polar radius measurements of the Sun reflect the polar limb brightening at this frequency.

To study the influence of changes in the equatorial atmosphere, the solar radius was determined again considering only the points with small deviations from the mean (±20″, ±15″, ±10″). These measurements showed a good correlation between the solar radius and the sunspot number before the year 1999, however after this year the solar radius diminishes while the sunspot number continues at an approximately constant value. This can be explained by the polar radius reduction after 1999, since the fits considering only points with small deviation contain a relatively larger fraction of polar points. That is, the more restrictive the selection criterion (smaller deviation), the larger the number of points in the equatorial region that are discarded. From our analysis, the quiet region in the neighborhood of the equator is filled with small sized bright structures that are responsible for the good correlation with the sunspot number. Figure 7 shows a comparison between a running mean taken every 100 days of the solar radius fitted considering points within ±30″, ±20″, ±15″, ±10″ deviations of the mean radius, plus the polar radius.

Table 1 displays the mean radius for different deviation criteria, the minimum and mean number of points used in the fits, the correlation coefficient between the radius variation and the sunspot number, and the last column shows the correlation coefficient between the radius variation and the North polar limb brightening. As the criterion becomes more conservative, a reduction in the mean solar radius is obtained tending to the polar radius value. Moreover, the correlation of radius with sunspot number is seen to decrease significantly until it becomes anti-correlated.

The mean radius values in Table 1 are smaller than those expected from previous measurements at other radio wavelengths (Bachurin 1983; Costa et al. 1985, 1999; Furst et al. 1979) where the radius was calculated at the point where the brightness temperature was half the value of the quiet Sun brightness temperature. Previous observations, however, were performed by single dish telescopes that have beams many times wider than the 10″ synthesized beam of the NoRH interferometer. The point at half the mean intensity is indeed the radius of the Sun only for the case where the Sun may be accurately described by a flat disc of constant intensity. Observation at radio frequencies greater than 10 GHz (Selhorst et al. 2003, and references therein) have shown the existence of solar limb

brightening. Thus, the calculation of the solar limb at half-intensity value is affected by the convolution with the telescope beam. The wider the beam, the larger the inferred radius in the presence of limb brightening.

Based on 1976 observations against 1980–81 measurements, Bachurin (1983) reported an increase in the solar radius of nearly 9.5 arcsec at 13 GHz and 13.8 arcsec at 8 GHz, while Costa et al. (1999) estimated an enlargement of 8 arcsec at 48 GHz based on more than 500 maps made during the 1991–93 period. Our work showed, in the present solar cycle, a variation in the solar radius from minimum to maximum solar activity periods. Changes of 3″ in the mean solar radius and 1″ in the polar radius were found. Besides the wider beams used in previous works, the discrepancy in the variation of the solar radius can be explained by the use of a small number of maps at different activity periods. Another cause may be that the studied period presented a sharp decrease (1991–93 in Costa et al. 1999) or increase (1997–99 in our work) that in a linear extrapolation could result in a wrong estimate of the total radius variation within a solar cycle.

4. Conclusions

The Nobeyama Radioheliograph has been an excellent source of solar studies since 1992. In this work, we have analyzed the solar radius temporal variations using daily maps at 17 GHz covering about one solar cycle (1992–2003).

The main results can be summarized as follows:

i) The overall mean solar radius varied from 976.6 ± 1.5 arcsec (30″ deviation) to 974.8 ± 0.6 (10″ deviation), whereas the mean polar radius was 974.4 ± 0.8.
ii) A strong correlation was found between the overall solar radius variation (30″ deviation) and the sunspot number, with a correlation coefficient of 0.88.
iii) The polar radius variation was found to be anti-correlated with the sunspot number (correlation coefficient of −0.64), but correlated with the polar limb brightening.
iv) A mean variation of 3 arcsec in the mean solar radius was found from minimum to maximum solar activity periods, whereas this variation was only 1″ for the polar radius.

Solar radius measurements at radio frequencies are not a simple task, because the Sun does not have a clear quiet atmosphere. This atmosphere is replete with ever-changing small structures (sunspots, proeminences, spicules, plages, faculae), that are prominent in the observed radio Sun. Moreover, these features influence the choice of where the solar radius is measured. If the atmosphere had a smooth profile, the brightest point at the solar limb would be close to the point where the optical depth is equal to unity at a certain frequency ($\tau_\nu = 1$). Selhorst et al. (2003), however, showed that the limb brightening intensity at 17 GHz is not uniformly distributed around the Sun, being larger near the polar region, indicating the influence of features such as spicules in the maximum brightening.

In most cases, the Sun radius is defined as the point where the brightness temperature is equal to half of the quiet Sun brightness temperature or as the inflection point. Both methods for measuring the mean solar and the polar radius described in this work, however, are influenced by the presence of atmospheric structures. Some of these features, like spicules, cannot be distinguished at the observed radio wavelength, because of the telescope's limited spatial resolution.

The measurement of variations in solar radius at radio frequencies represent a global indicator of solar atmospheric changes, and with other solar indicators can provide better models for the Sun's atmosphere. For future work we propose to extend the study of solar radius variations at 17 GHz for longer periods of time to other activity cycles and to other frequencies with high angular resolution. These will improve the understanding of how atmospheric features influence the solar radius at different heights.

Acknowledgements. We are grateful to the NoRH staff for obtaining the full disk 17 GHz maps and making them available over the Internet, and also to NOAA for providing sunspot number data. The Nobeyama Radioheliograph is operated by NAOJ/Nobeyama Solar Radio Observatory. C.L.S. acknowledges financial support from the Brazilian agency FAPESP, grant number 01/02106-3.

References

Antia, H. M. 1998, A&A, 330, 336
Bachurin, A. F. 1983, Izvestiia, 68, 68
Brown, T. M., & Christensen-Dalsgaard, J. 1998, ApJ, 500, L195
Costa, J. E. R., Silva, A. V. R., Makhmutov, V. S., et al. 1999, ApJ, 520, L63
Costa, J. E. R., Homor, J. L., & Kaufmann, P. 1985, in Solar Flares and Coronal Physics Using P/OF as a Research Tool (NASA-CP 2421) (Huntsville: NASA), 201
Delache, Ph., Gavriusev, V., Gavriuseva, E., et al. 1993, ApJ, 407, 801
Emilio, M., Kuhn, J. R., Bush, R. I., & Scherrer, P. 2000, ApJ, 543, 1007
Furst, E., Hirth, W., & Lantos, P. 1979, Sol. Phys., 63, 257
Gilliland, R. L. 1981, ApJ, 248, 1144
Laclare, F., Delmas, C., Coin, J. P., & Irbah, A. 1996, Sol. Phys., 166, 211
Nakajima, H., Nishio, M., Enome, S., et al. 1994, Proc. IEEE, 82, 705
Neckel, H. 1995, Sol. Phys., 156, 7
Rozelot, J. P. 1998, Sol. Phys., 177, 321
Selhorst, C. L., Silva, A. V. R., Costa, J. E. R., & Shibasaki, K. 2003, A&A, 401, 1143
Shibasaki, K. 1998, in Synoptic Solar Physics, ed. K. S. Balasubramaniam, J. Harvey, & D. Rabin, ASP Conf. Ser., 140, 373
Ulrich, R. K., & Bertello, L. 1995, Nature, 377, 214
Wittmann, A. D., Alge, E., & Bianda, M. 1993, Sol. Phys., 205, 206